Universität Potsdam

Fred Feudel, Norbert Seehafer, Olaf Schmidtmann

Bifurcation phenomena of the magnetofluid equations

NLD Preprints ; 9

Bifurcation phenomena of the magnetofluid equations

Fred Feudel, Norbert Seehafer and Olaf Schmidtmann
Max-Planck-Gruppe Nichtlineare Dynamik, Universität Potsdam, PF 601553, D-14415 Potsdam, Germany

Abstract

We report on bifurcation studies for the incompressible magnetohydrodynamic equations in three space dimensions with periodic boundary conditions and a temporally constant external forcing. Fourier representations of velocity, pressure and magnetic field have been used to transform the original partial differential equations into systems of ordinary differential equations (ODE), to which then special numerical methods for the qualitative analysis of systems of ODE have been applied, supplemented by the simulative calculation of solutions for selected initial conditions. In a part of the calculations, in order to reduce the number of modes to be retained, the concept of approximate inertial manifolds has been applied. For varying (increasing from zero) strength of the imposed forcing, or varying Reynolds number, respectively, time-asymptotic states, notably stable stationary solutions, have been traced. A primary non-magnetic steady state loses, in a Hopf bifurcation, stability to a periodic state with a non-vanishing magnetic field, showing the appearance of a generic dynamo effect. From now on the magnetic field is present for all values of the forcing. The Hopf bifurcation is followed by further, symmetry-breaking, bifurcations, leading finally to chaos. We pay particular attention to kinetic and magnetic helicities. The dynamo effect is observed only if the forcing is chosen such that a mean kinetic helicity is generated; otherwise the magnetic field diffuses away, and the time-asymptotic states are non-magnetic, in accordance with traditional kinematic dynamo theory.

1. Introduction

A prominent objective in the theory of electrically conducting fluids is the explanation of the origin of the cosmical magnetic fields, such as those of the Earth and the Sun (for a recent account of the subject see e.g. Ref. [18]). The majority of studies in this field has been kinematic. Kinematic dynamo theory studies the conditions under which a prescribed velocity field can amplify, or at least prevent from decaying, some seed magnetic field, completely disregarding the equations governing the motion of the fluid. The hitherto most successful branch of kinematic dynamo theory is the theory of the turbulent dynamo [9, 13, 15, 21]. The central mechanism in this theory is the generation of a mean, or large-scale, electromotive force by turbulently fluctuating, or small-scale, parts of velocity and magnetic field. It has been found that the presence of kinetic and magnetic helicities is favourable for a turbulent dynamo effect. With $\mathbf{v}$, $\mathbf{B}$ and $\mathbf{A}$ denoting fluid velocity, magnetic field

and a magnetic vector potential, the densities per unit volume of kinetic, magnetic and current helicity are defined by

$$H_K = \mathbf{v} \cdot \operatorname{curl} \mathbf{v}; \quad H_M = \mathbf{A} \cdot \mathbf{B}; \quad H_C = \mathbf{B} \cdot \operatorname{curl} \mathbf{B}. \tag{1}$$

Simple examples of strongly helical flows are provided by the so-called ABC flows (named after Arnold, Beltrami and Childress),

$$\mathbf{v} = \mathbf{v}_{ABC} = (A \sin z + C \cos y,\ B \sin x + A \cos z,\ C \sin y + B \cos x), \tag{2}$$

where A, B and C denote constant coefficients. By satisfying $\operatorname{curl} \mathbf{v} = \mathbf{v}$, they have the Beltrami property, $\operatorname{curl} \mathbf{v} \times \mathbf{v} = \mathbf{0}$, and in general (if $ABC \neq 0$), there are domains in the flow where the streamlines are chaotic. For these reasons, they have received much interest [2, 3, 7], notably as candidates for fast dynamos (kinematic dynamos for which the growth rate of the magnetic field remains bounded away from zero as the magnetic diffusivity tends to zero). The ABC flows are steady solutions of the incompressible (constant density) Euler equations. They are also steady solutions of the incompressible Navier–Stokes equations (NSE) if an external body force

$$\mathbf{f} = -\nu \Delta \mathbf{v}_{ABC} = \nu \mathbf{v}_{ABC} \tag{3}$$

just compensating for viscous losses (see Eq. (4) below) is applied; in this case they are stable below und unstable above a certain critical strength of the forcing or critical Reynolds number, respectively [8, 16].

Imposing this kind of forcing, Galanti et al. [6] studied the complete system of the (incompressible) magnetohydrodynamic (MHD) equations. Numerically simulating the system for selected Reynolds numbers and selected initial conditions, they observed that at some critical value of the Reynolds number a stable ABC flow without magnetic field loses stability to a time-periodic state with a magnetic field. In the present paper we continue the study of Galanti et al. by systematically applying numerical methods of bifurcation analysis. By applying an alternative forcing with zero mean helicity, we also test the role of helicity for a dynamo effect.

In Sect. 2 we cast the 3D MHD equations, which contain the 3D NSE as a special case, into spectral form and explain the kind of truncation used, while Sect. 3 deals with the applied external forcing and the symmetries of the system associated with it. Then in Sects. 4 and 5 we present the results of our calculations, namely in Sect. 4 a bifurcation sequence leading to chaos for the ABC forcing (Eq. (3)) and in Sect. 5 results for our alternative forcing.

2. Basic equations and truncation

We start from the equations for a non-relativistic, incompressible, electrically conducting fluid with constant material properties (cf. e.g. Roberts [17]),

$$\frac{\partial \mathbf{v}}{\partial t} + (\mathbf{v} \cdot \nabla)\mathbf{v} = \nu \Delta \mathbf{v} - \operatorname{grad} p - \frac{1}{2} \operatorname{grad} \mathbf{B}^2 + (\mathbf{B} \cdot \nabla)\mathbf{B} + \mathbf{f}, \tag{4}$$

$$\frac{\partial \mathbf{B}}{\partial t} + (\mathbf{v}\cdot\nabla)\mathbf{B} = \eta\Delta\mathbf{B} + (\mathbf{B}\cdot\nabla)\mathbf{v}, \tag{5}$$

$$\operatorname{div}\mathbf{v} = 0, \quad \operatorname{div}\mathbf{B} = 0, \tag{6}$$

where $\mathbf{v}$, p, and $\mathbf{B}$ denote fluid velocity, thermal pressure, and magnetic field, ν and η the kinematic viscosity and magnetic diffusivity, respectively, and $\mathbf{f}$ is a yet unspecified body force. The third and fourth terms on the right of Eq. (4) constitute the Lorentz force.

We apply periodic boundary conditions on a cube of side length 2π, which is equivalent to considering the motion on the torus $T^3 = [0,2\pi]\times[0,2\pi]\times[0,2\pi]$. The mean values of $\mathbf{v}$ and $\mathbf{B}$, and consequently also of $\mathbf{f}$, are assumed to vanish,

$$\int_{T^3} \mathbf{v}\,\mathrm{d}^3\mathbf{x} = \mathbf{0}, \quad \int_{T^3} \mathbf{B}\,\mathrm{d}^3\mathbf{x} = \mathbf{0}, \quad \int_{T^3} \mathbf{f}\,\mathrm{d}^3\mathbf{x} = \mathbf{0}. \tag{7}$$

The periodicity assumption implies that the Fourier representations of $\mathbf{v}$, $\mathbf{B}$, p and $\mathbf{f}$,

$$\mathbf{v}(\mathbf{x}) = \sum_{\substack{\mathbf{k}\in\mathbb{Z}^3\\ \mathbf{k}\neq\mathbf{0}}} \mathbf{v}_\mathbf{k}\exp(\mathrm{i}\mathbf{k}\cdot\mathbf{x}), \quad \mathbf{B}(\mathbf{x}) = \sum_{\substack{\mathbf{k}\in\mathbb{Z}^3\\ \mathbf{k}\neq\mathbf{0}}} \mathbf{B}_\mathbf{k}\exp(\mathrm{i}\mathbf{k}\cdot\mathbf{x}), \tag{8}$$

$$p(\mathbf{x}) = \sum_{\mathbf{k}\in\mathbb{Z}^3} p_\mathbf{k}\exp(\mathrm{i}\mathbf{k}\cdot\mathbf{x}), \quad \mathbf{f}(\mathbf{x}) = \sum_{\substack{\mathbf{k}\in\mathbb{Z}^3\\ \mathbf{k}\neq\mathbf{0}}} \mathbf{f}_\mathbf{k}\exp(\mathrm{i}\mathbf{k}\cdot\mathbf{x}), \tag{9}$$

can be differentiated term by term with respect to the spatial coordinates. In Fourier space Eq. (6) takes the form

$$\mathbf{v}_\mathbf{k}\cdot\mathbf{k} = 0, \quad \mathbf{B}_\mathbf{k}\cdot\mathbf{k} = 0 \tag{10}$$

and is automatically satisfied if we write

$$\mathbf{v}_\mathbf{k} = v_\mathbf{k}^{(1)}\mathbf{e}_\mathbf{k}^{(1)} + v_\mathbf{k}^{(2)}\mathbf{e}_\mathbf{k}^{(2)}, \quad \mathbf{B}_\mathbf{k} = B_\mathbf{k}^{(1)}\mathbf{e}_\mathbf{k}^{(1)} + B_\mathbf{k}^{(2)}\mathbf{e}_\mathbf{k}^{(2)} \qquad \text{for } \mathbf{k}\neq\mathbf{0}, \tag{11}$$

with (real) "polarization" unit vectors $\mathbf{e}_\mathbf{k}^{(1)}$, $\mathbf{e}_\mathbf{k}^{(2)}$ perpendicular to $\mathbf{k}$,

$$\mathbf{e}_\mathbf{k}^{(i)}\cdot\mathbf{k} = 0, \quad \mathbf{e}_\mathbf{k}^{(1)}\cdot\mathbf{e}_\mathbf{k}^{(2)} = 0, \quad \mathbf{e}_\mathbf{k}^{(i)}\cdot\mathbf{e}_\mathbf{k}^{(i)} = 1, \quad \mathbf{e}_{-\mathbf{k}}^{(i)} = \mathbf{e}_\mathbf{k}^{(i)}, \qquad i = 1,2. \tag{12}$$

The last condition in Eq. (12) ensures that

$$v_{-\mathbf{k}} = v_\mathbf{k}^*, \quad B_{-\mathbf{k}} = B_\mathbf{k}^* \tag{13}$$

for real $\mathbf{v}(\mathbf{x})$ and $\mathbf{B}(\mathbf{x})$ (an asterisk indicates the complex conjugate). By using these representations for $\mathbf{v}_\mathbf{k}$ and $\mathbf{B}_\mathbf{k}$ we furthermore easily get rid of both the thermal, $\operatorname{grad} p$, and magnetic, $\operatorname{grad}\mathbf{B}^2/2$, pressure terms in Eq. (4) and arrive at the following infinite-dimensional system of ODE:

$$\frac{\mathrm{d}v_\mathbf{k}^{(j)}}{\mathrm{d}t} = -\nu\mathbf{k}^2 v_\mathbf{k}^{(j)} - \mathrm{i}\sum_{\substack{\mathbf{p}\in\mathbb{Z}^3\\ \mathbf{p}\neq\mathbf{0},\mathbf{k}}}\sum_{\alpha,\beta=1}^{2} (\mathbf{e}_\mathbf{p}^{(\alpha)}\cdot\mathbf{e}_\mathbf{k}^{(j)})(\mathbf{e}_{\mathbf{k}-\mathbf{p}}^{(\beta)}\cdot\mathbf{k})[v_\mathbf{p}^{(\alpha)}v_{\mathbf{k}-\mathbf{p}}^{(\beta)} - B_\mathbf{p}^{(\alpha)}B_{\mathbf{k}-\mathbf{p}}^{(\beta)}] + f_\mathbf{k}^{(j)}, \tag{14}$$

$$\frac{\mathrm{d}B_{\mathbf{k}}^{(j)}}{\mathrm{d}t} = -\eta\mathbf{k}^2 B_{\mathbf{k}}^{(j)} - \mathrm{i}\sum_{\substack{\mathbf{p}\in\mathbb{Z}^3\\ \mathbf{p}\neq\mathbf{0},\mathbf{k}}}\sum_{\alpha,\beta=1}^{2}(\mathbf{e}_{\mathbf{p}}^{(\alpha)}\cdot\mathbf{e}_{\mathbf{k}}^{(j)})(\mathbf{e}_{\mathbf{k}-\mathbf{p}}^{(\beta)}\cdot\mathbf{k})[B_{\mathbf{p}}^{(\alpha)}v_{\mathbf{k}-\mathbf{p}}^{(\beta)} - v_{\mathbf{p}}^{(\alpha)}B_{\mathbf{k}-\mathbf{p}}^{(\beta)}]. \quad (15)$$

$f_{\mathbf{k}}^{(j)}$ on the right of Eq. (14) is defined by

$$f_{\mathbf{k}}^{(j)} = \mathbf{f}_{\mathbf{k}}\cdot\mathbf{e}_{\mathbf{k}}^{(j)}, \qquad j = 1, 2. \quad (16)$$

In our numerical calculations, we have used an isotropic truncation in wave number space, following Lee [10, 11], who segmented $\mathbf{k}$ space into successive shells $n^2 - n < \mathbf{k}^2 \leq n^2 + n$, $n = 1, 2, \cdots$. In most of our calculations we have taken into account three shells, corresponding to 89 $\mathbf{k}$-vectors, which amounts to studying a system of 712 ODE. But partially, to test the influence of the degree of truncation, up to 9 shells were included in the computations, corresponding to 1847 $\mathbf{k}$-vectors and 14776 ODE, respectively.

In order to improve for a given truncation the quality of the approximation, we also used the concept of approximate inertial manifolds (AIMs) [4, 5, 20] in a part of the calculations. An inertial manifold (IM) represents, in the form of a map $z = \phi(y)$, an exact interaction law between the small-scale components z (also called slaved modes) and the large-scale components y of a solution to an infinite-dimensional dynamical system. The existence of an IM for the 3D MHD equations, as also for the 3D NSE, is an open question. Generalizing methods developed for the NSE [20], we have constructed and used in place of ϕ an AIM $\hat{\phi}$, a map representing the modes belonging to higher-order shells in $\mathbf{k}$ space by those belonging to lower-order shells.

3. Forcing and symmetries

Because of the periodic boundary conditions, the total energy flow through the boundary of our cube vanishes, so that in order to compensate for viscous and ohmic losses some kind of external forcing has to be applied. We have used a forcing according to Eqs. (3) and (2) with

$$A = B = C = f. \quad (17)$$

For this forcing the MHD equations are equivariant with respect to a discrete symmetry group which contains 24 elements and is isomorphic to the octaeder group O (the rotation group of the cube) [1, 3]. A number of bifurcations observed in the system are related to these symmetries.

Let a prime denote transformed quantities. Each symmetry transformation T is a combination of a rigid rotation with a translation and can be written as

$$\mathbf{x}' = \mathrm{T}\mathbf{x} = \mathrm{D}\mathbf{x} + \mathbf{a}, \quad (18)$$

where D is an orthogonal 3×3 matrix and $\mathbf{a}$ a constant vector. The whole symmetry group is, for instance, generated by the two transformations

$$\mathrm{T}_1: \qquad \mathrm{D} = \begin{pmatrix} 1 & 0 & 0 \\ 0 & 0 & 1 \\ 0 & -1 & 0 \end{pmatrix}, \quad \mathbf{a} = \frac{1}{2}\begin{pmatrix} \pi \\ -\pi \\ \pi \end{pmatrix} \quad (19)$$

and

$$\mathrm{T}_2: \qquad \mathrm{D} = \begin{pmatrix} 0 & 0 & -1 \\ 0 & 1 & 0 \\ 1 & 0 & 0 \end{pmatrix}, \quad \mathbf{a} = \frac{1}{2}\begin{pmatrix} \pi \\ \pi \\ -\pi \end{pmatrix}. \tag{20}$$

Associated with the transformation of the position vector $\mathbf{x}$ given by Eq. (18) is a transformation of the vector field $\mathbf{v}(\mathbf{x})$ ($\mathbf{B}(\mathbf{x})$ is transformed in the same way) according to

$$\mathbf{v}'(\mathbf{x}) = \mathrm{D}\mathbf{v}(\mathrm{T}^{-1}\mathbf{x}). \tag{21}$$

In Fourier space Eq. (21) takes the form

$$\mathbf{v}'_{\mathbf{k}} = \mathrm{D}\mathbf{v}_{\tilde{\mathbf{k}}} \cdot \exp(-\mathrm{i}\mathbf{k}\cdot\mathbf{a}), \tag{22}$$

where

$$\tilde{\mathbf{k}} = \mathrm{D}^{-1}\mathbf{k}, \tag{23}$$

and for the quantities $v^{(1)}_{\mathbf{k}}$ and $v^{(2)}_{\mathbf{k}}$ one obtains

$$v'^{(j)}_{\mathbf{k}} = \exp(-\mathrm{i}\mathbf{k}\cdot\mathbf{a}) \sum_{\alpha=1}^{2} v^{(\alpha)}_{\tilde{\mathbf{k}}} (\mathrm{D}\mathbf{e}^{(\alpha)}_{\tilde{\mathbf{k}}}) \cdot \mathbf{e}^{(j)}_{\mathbf{k}}. \tag{24}$$

By using this relation (and the corresponding one for the magnetic field) it can be checked with respect to which transformations of the symmetry group, if any, a particular solution is symmetric, provided this solution is sufficiently regular, for example time-periodic.

Following Galanti et al. [6], we have defined kinetic and magnetic Reynolds numbers R and Rm by

$$R = \frac{f}{\nu}, \quad Rm = \frac{f}{\eta}. \tag{25}$$

While restricting ourselves to the case $\nu = \eta$ (magnetic Prandtl number equal to unity), R has been our bifurcation parameter.

In order to test the role played by helicity, alternatively also a forcing in the form

$$\mathbf{f} = \frac{\nu}{2}(\mathbf{v}_{ABC} + \mathbf{v}^{-}_{ABC}) \tag{26}$$

with

$$\mathbf{v}^{-}_{ABC} = (-A\cos z - C\sin y,\ -B\cos x - A\sin z,\ -C\cos y - B\sin x) \tag{27}$$

has been applied. $\mathbf{v}^{-}_{ABC}$ satisfies $\mathrm{curl}\,\mathbf{v}^{-}_{ABC} = -\mathbf{v}^{-}_{ABC}$, and its addition in the forcing term "kills" the helicity on average in the volume. Namely,

$$\begin{aligned} &\mathrm{curl}(\mathbf{v}_{ABC} + \mathbf{v}^{-}_{ABC}) \cdot (\mathbf{v}_{ABC} + \mathbf{v}^{-}_{ABC}) \\ &= \mathbf{v}^2_{ABC} - (\mathbf{v}^{-}_{ABC})^2 \\ &= 2[\sin(z-y) + \sin(x-z) + \sin(y-x)]. \end{aligned} \tag{28}$$

4. Bifurcation sequence for ABC forcing

The results presented now refer to the positive-helicity forcing given by Eq. (3).

For weak forcing (small R), there exists a stable stationary solution, namely the ABC flow (given by Eq. (2)) with vanishing magnetic field, and all system trajectories are attracted by this solution, which is symmetric with respect to all the 24 transformations of the symmetry group O. For varying R, we have traced the steady-solution branch by means of a predictor-corrector method. Thereby in each step, in order to detect bifurcation points, the eigenvalues of the Jacobian matrix have been calculated. The steady state loses stability in a Hopf bifurcation, leading to a periodic solution with a magnetic field as the only time-asymptotic state. Table 1 summarizes the values of the Reynolds number at which the Hopf bifurcation

Number of shells in **k** space	Number of modes (equations)	Critical R for Hopf bifurcation
2	40 (320)	4.6
3	89 (712)	5.7
4	194 (1552)	12.7
5	369 (2952)	8.2
6	594 (4752)	<12.5
7	895 (7160)	<11.0
9	1847 (14776)	<12.0
3/1	89/105 (712)	7.5
3/2	89/280 (712)	7.6
3/3	89/505 (712)	8.0
4/1	194/175 (1552)	7.8
4/2	194/400 (1552)	9.2
4/3	194/701 (1552)	9.6
4/4	194/1082 (1552)	10.0

Table 1: Reynolds number at which the Hopf bifurcation was observed for different truncations in wave number space. The lower part refers to the inertial-manifold method (see text).

appeared for different truncations. The upper part of the table gives the values for ordinary truncation in Fourier space, whereas in the lower part results obtained by using the inertial-manifold method are represented, the two numbers in columns 1 and 2 referring to non-slaved (first number) and slaved modes, respectively.

Discernible in Table 1 is a dependence of the critical Reynolds number on the degree of truncation, with a tendency to higher values for weaker truncation. The latter may be due to an increase of the energy dissipation with increasing number of modes.

Because of a very long run time of the program calculating the eigenvalues of the Jacobian matrix, for the cases with more than 5 shells in $\mathbf{k}$ space only upper bounds for the critical Reynolds number are given, obtained from simulations of single trajectories.

Quite generally, the ordinary-truncation and inertial-manifold methods revealed identical generic bifurcation properties of the system. Merely shifts of the bifurcation values of R were observed between the two methods. The case "4/1" in Table 1 may serve as an example of how the inertial-manifold method takes into account the influence of the exterior shells (slaved modes): The relatively low value of the critical Reynolds compared to the four-shell case in ordinary truncation reflects the destabilizing influence of the fifth shell (see upper part of table).

In the following we present results obtained by applying the (simple) three-shell truncation. Since the Hopf bifurcation leading to a dynamo effect seems to be generic, these results are likely to be representative of the system at least for Reynolds numbers not too far above the Hopf value.

In Fig. 1 the instability of the ABC flow is demonstrated for a Reynolds number

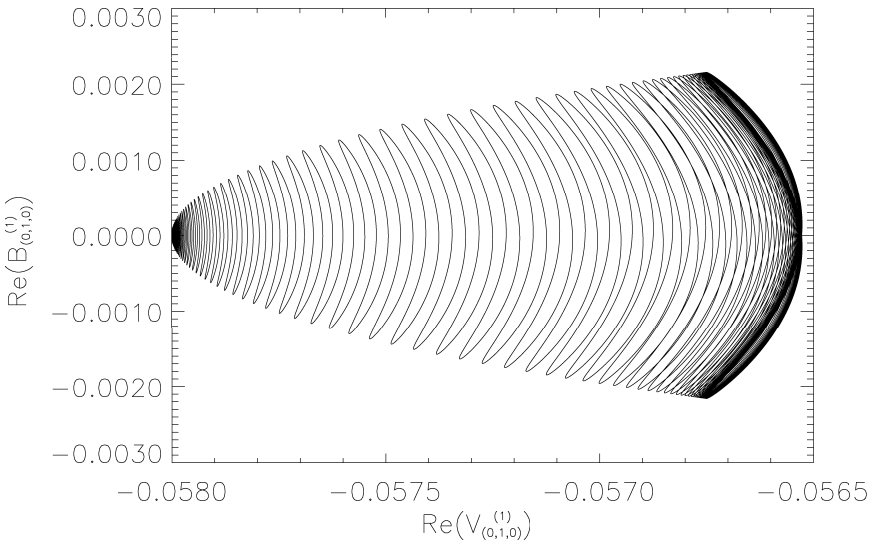

Figure 1: Example of a trajectory demonstrating the instability of the primary steady state after the Hopf bifurcation for $R = 5.8$.

only slightly above the Hopf value. It can be seen how a trajectory escapes the originally stable fixed point and approaches a periodic orbit.

The Hopf bifurcation is non-degenerate. Just one pair of complex conjugate eigenvalues crosses the imaginary axis, the derivative of their real part with respect to R being different from zero thereby. Consequently just one periodic solution originates, which is still symmetric with respect to the full group O. But for $R = 7.7$ three new stable periodic solutions appear, which can be transformed into each other

by certain elements of O. The three new solutions do not bifurcate from the stable symmetric cycle, which coexists with them. We suppose that they are generated in (due to the symmetry simultaneous) saddle-node bifurcations.

For $R = 11.55$ also the symmetric branch loses part of its symmetry. The cycle bifurcates into four new periodic solutions, which can be be transformed into one another by elements of O. Thus now altogether 7 stable periodic solutions coexist.

Both branches, the four-solutions one and the three-solutions one, lead finally to chaotic states if R is further increased. Here we describe the transition for the three-solutions branch. In a second Hopf bifurcation at $R = 16$ a torus solution, as shown in Fig. 2, is generated (more precisely: three stable tori, namely from each of

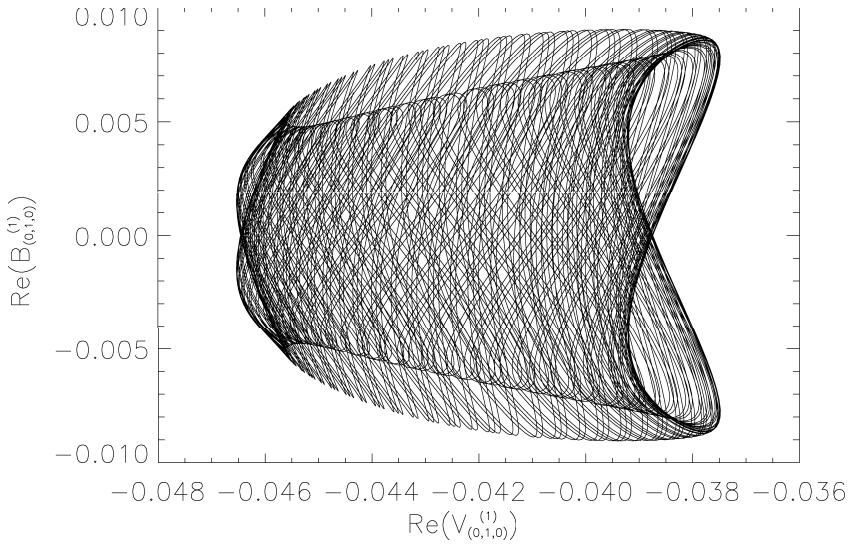

Figure 2: Torus solution for $R = 16$.

the three periodic solutions of the considered branch just one). At $R = 20$ the torus decays to a chaotic attractor, depicted in Fig. 3. The appearance of chaos has been verified by calculating the 5 largest Lyapunov exponents. For this calculation we have used the algorithm of Shimada and Nagashima [19]. Fig. 4 shows the Lyapunov exponents in dependence on the integration time. A good convergence is discernible, as well as that at least the largest exponent is positive.

After the first Hopf bifurcation the magnetic energy increases to a value of about 10 % of the total energy. A similar ratio between magnetic and kinetic energies was observed by Meneguzzi et al. [12] in 3D MHD simulation experiments.

We have also calculated relative kinetic and magnetic helicities $\hat{H}_K$ and $\hat{H}_M$ as defined by Galanti et al. [6],

$$\hat{H}_K = \frac{\int_{T^3} \mathbf{v} \cdot \operatorname{curl} \mathbf{v} \, \mathrm{d}^3\mathbf{x}}{\sqrt{\int_{T^3} \mathbf{v}^2 \, \mathrm{d}^3\mathbf{x} \int_{T^3} (\operatorname{curl} \mathbf{v})^2 \, \mathrm{d}^3\mathbf{x}}}, \quad \hat{H}_M = \frac{\int_{T^3} \mathbf{A} \cdot \mathbf{B} \, \mathrm{d}^3\mathbf{x}}{\sqrt{\int_{T^3} \mathbf{A}^2 \, \mathrm{d}^3\mathbf{x} \int_{T^3} \mathbf{B}^2 \, \mathrm{d}^3\mathbf{x}}}, \tag{29}$$

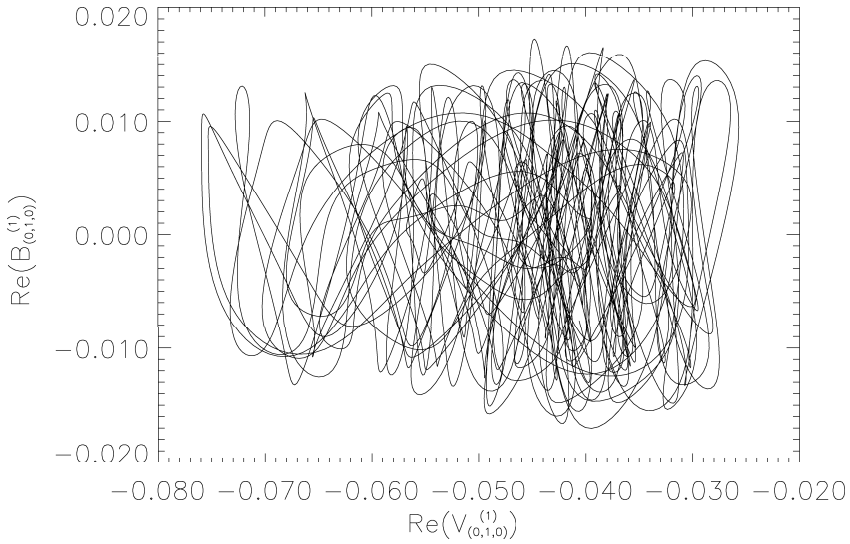

Figure 3: Trajectory on chaotic attractor for $R = 20$.

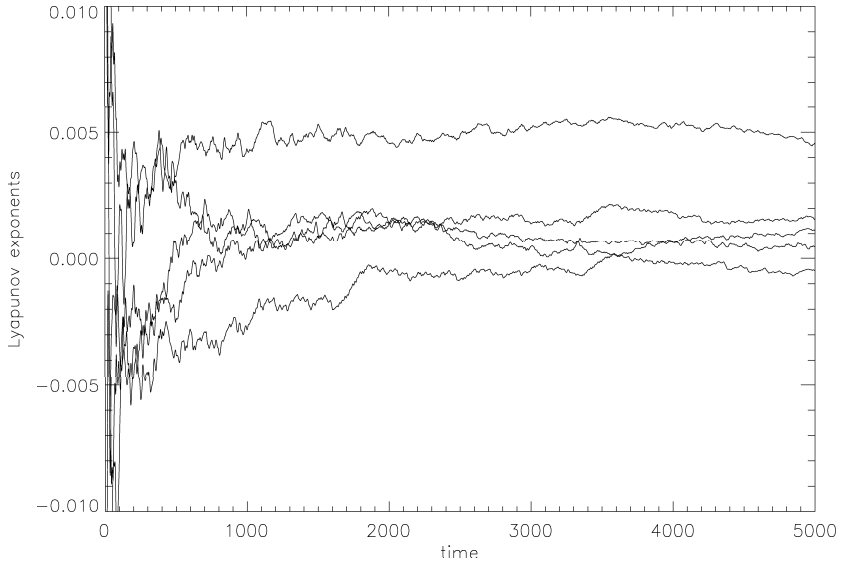

Figure 4: The 5 largest Lyapunov exponents versus integration time for $R = 20$.

and found that they depend on the Reynolds number only very weakly. In the time-periodic states both are constant in time, the value of $\hat{H}_K$ being slightly decreased compared to that in the non-magnetic state ($\hat{H}_M$ is not defined in the non-magnetic state).

5. Results for forcing with zero mean helicity

When applying the forcing given by Eq. (26), for small Reynolds numbers again a stable non-magnetic steady solution was found. At $R = 16$ the steady-solution branch loses stability in a probably degenerate bifurcation. Two real eigenvalues pass extremely slowly through zero. Above the bifurcation value for R an only very weakly attractive stable periodic solution with vanishing magnetic field was found, followed, for further increased R, by an apparently chaotic, also non-magnetic solution, as depicted in projection to a plane in Fig. 5. The form of the trajectory is

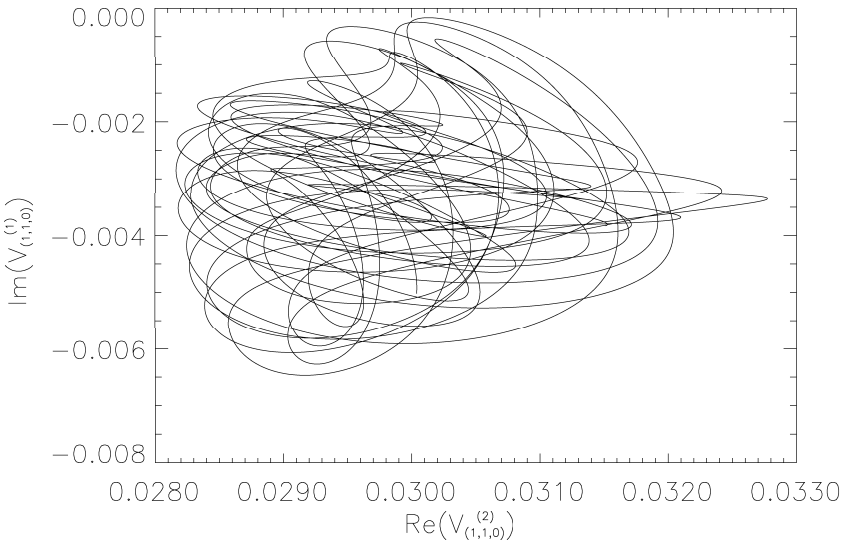

Figure 5: Trajectory for forcing with zero mean helicity at $R = 18.5$.

reminiscent of a textbook picture of Shilnikov chaos (see e.g. Ref. [14]), which is the result of a global bifurcation. However, this problem, as well as the character of the first bifurcation of the primary steady state, are still under investigation presently.

For the zero-mean-helicity forcing we never observed a dynamo effect. This has been checked by simulations up to $R = 80$. As shown in an example in Fig. 6, any initial magnetic field diffuses away. This seems to confirm results from traditional kinematic mean-field dynamo theory.

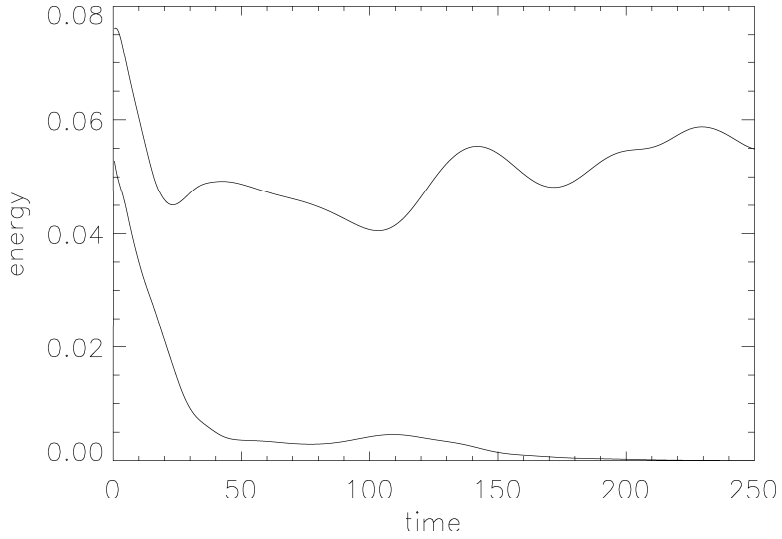

Figure 6: Example of the evolution of kinetic (upper curve) and magnetic energies for zero-mean-helicity forcing ($R = 13.5$).

References

[1] V. I. Arnold. On the evolution of a magnetic field under the influence of advection and diffusion (in Russian). In V.M. Tikhomirov, editor, *Some Problems of Modern Analysis*, pages 8–21. Moscow State University, 1984.

[2] V. I. Arnold and E. I. Korkina. The growth of a magnetic field in a three-dimensional steady incompressible flow (in Russian). *Vest. Mosk. Univ. Mat. Mekh.*, 3, 43–46, 1983.

[3] T. Dombre, U. Frisch, J. M. Greene, M. Hénon, A. Mehr, and A. M. Soward. Chaotic streamlines in the ABC flows. *J. Fluid Mech.*, 167, 353–391, 1986.

[4] C. Foias, B. Nicolaenko, G. R. Sell, and R. Temam. Inertial manifolds for the Kuramoto–Sivashinsky equation and an estimate of their lowest dimension. *J. Math. Pures Appl.*, 67, 197–226, 1988.

[5] C. Foias, G. R. Sell, and R. Temam. Inertial manifolds for nonlinear evolutionary equations. *J. Diff. Eq.*, 73, 309–353, 1988.

[6] B. Galanti, P. L. Sulem, and A. Pouquet. Linear and non-linear dynamos associated with ABC flows. *Geophys. Astrophys. Fluid Dyn.*, 66, 183–208, 1992.

[7] D. Galloway and U. Frisch. Dynamo action in a family of flows with chaotic streamlines. *Geophys. Astrophys. Fluid Dyn.*, 36, 53–83, 1986.

[8] D. Galloway and U. Frisch. A note on the stability of a family of space-periodic Beltrami flows. *J. Fluid Mech.*, 180, 557–564, 1987.

[9] F. Krause and K.-H. Rädler. *Mean-Field Magnetohydrodynamics and Dynamo Theory.* Akademie-Verlag, Berlin, 1980.

[10] J. Lee. Steady-state simulation of 2D homogeneous turbulence. *Physica D*, 37, 417–422, 1989.

[11] J. Lee. Topology of trajectories of the 2D Navier–Stokes equations. *Chaos*, 2, 537–563, 1992.

[12] M. Meneguzzi, U. Frisch, and A. Pouquet. Helical and non-helical turbulent dynamos. *Phys. Rev. Lett.*, 47, 1060–1064, 1981.

[13] H. K. Moffatt. *Magnetic Field Generation in Electrically Conducting Fluids.* Cambridge Univ. Press, Cambridge, 1978.

[14] G. Nicolis and P. Gaspard. Bifurcations, chaos and self-organisation in reaction-diffusion systems. In D. Roose, B. de Dier, and A. Spence, editors, *Continuations and Bifurcations: Numerical Techniques and Applications*, pages 43–70. Kluwer, Dordrecht, 1990.

[15] E. N. Parker. *Cosmical Magnetic Fields.* Clarendon Press, Oxford, 1979.

[16] O. Podvigina and A. Pouquet. On the non-linear stability of the 1:1:1 ABC flow. *Physica D*, 75, 471–508, 1994.

[17] P. H. Roberts. *An Introduction to Magnetohydrodynamics.* Longmans, London, 1967.

[18] P. H. Roberts and A. M. Soward. Dynamo theory. *Ann. Rev. Fluid Mech.*, 24, 459–512, 1992.

[19] I. Shimada and T. Nagashima. A numerical approach to ergodic problem of dissipative dynamical systems. *Progr. Theor. Phys.*, 61, 1605–1616, 1979.

[20] E. S. Titi. On approximate inertial manifolds to the Navier–Stokes equations. *J. Math. Anal. Appl.*, 149, 540–557, 1990.

[21] Ya.B. Zeldovich, A. A. Ruzmaikin, and D. D. Sokoloff. *Magnetic Fields in Astrophysics.* Gordon and Breach, New York, 1983.